ELSEVIER

Journal of Nuclear Materials 290–293 (2001) 71–75

journal of nuclear materials

www.elsevier.nl/locate/jnucmat

Formation of mixed layers and compounds on beryllium due to C^+ and CO^+ bombardment

P. Goldstrass [1], Ch. Linsmeier *

Max-Planck-Institut für Plasmaphysik, EURATOM Association, Boltzmannstr. 2, Garching D-85748, Germany

Abstract

Compound formation on a clean beryllium single crystal (0 0 0 1) during bombardment with 5 keV C^+ and 3 and 5 keV CO^+ ions is studied by means of in situ X-ray photoelectron spectroscopy (XPS). In combination with in situ Rutherford backscattering analysis (RBS), TRIDYN computer simulation, and measurements of the weight change of the sample due to the bombardment, models for the sample composition changes and erosion mechanisms are derived for both ion species. In the case of C^+ bombardment a carbon layer builds up on top of the beryllium. The transition region from pure beryllium to pure carbon consists partly of Be_2C and the beryllium erosion stops as the covering carbon layer develops. During CO^+ bombardment a deposition/erosion equilibrium is established. After initial C and O accumulation, the beryllium substrate is covered by a ternary mixture layer of about 10 nm thickness containing BeO, elementary carbon and C–O compounds. Be_2C is present only at low fluences and before the equilibrium is established. The erosion of beryllium proceeds and a chemical erosion process limits the deposited amounts of carbon and oxygen via emission of CO.

Keywords: Beryllium; Carbon; Beryllium carbide; Erosion; Ion irradiation

1. Introduction

In present experiments and in the design of future fusion plasma devices like ITER, several elements are being considered as first wall materials [1]. This use of multiple materials and the presence of impurities in the plasma (e.g., oxygen) will result in the formation of mixed materials at the first wall because of erosion and (re-) deposition during the discharges. The use of multiple materials in JET has led to a considerable improvement of the plasma performance and the hydrogen inventory of the first wall [2–5]. Carbon has been used in most fusion machines and both carbon and beryllium are candidate first wall materials for ITER [1].

Earlier investigations showed that in the case of C^+ bombardment of beryllium, a carbon adlayer builds up on top of the substrate and protects the beryllium from further erosion. In the case of CO^+ bombardment (simulating an oxygen and carbon co-bombardment) a deposition/erosion equilibrium is established. This cannot be explained assuming physical sputtering to be the only erosion mechanism [6]. In this paper the chemical interactions between the different elements in these mixed materials are studied to develop deposition/erosion models for both ion species.

2. Experiment

A polished beryllium single crystal (0 0 0 1) was cleaned by 1 keV Ar^+ sputtering and bombarded with 5 keV C^+ and 5 keV CO^+ at normal incidence in the new UHV experiment ARTOSS [7]. After the cleaning process the only detectable impurity was oxygen (X-ray photoelectron spectroscopy (XPS) measurement:

* Corresponding author. Tel.: +49-89 3299 2285; fax: +49-89 3299 2279.

E-mail addresses: peter.goldstrass@ipp.mpg.de (P. Goldstrass), linsmeier@ipp.mpg.de (C. Linsmeier).

[1] Tel.: +49-89 3299 1497; fax: +49-89 3299 1149.

0022-3115/01/$ - see front matter
PII: S0022-3115(00)00618-8

$<10^{14}$ cm^{-2}). The oxygen contamination did not exceed this value during the implantation experiments. Both ion species were supplied by a Colutron type ion source using CO_2 as a precursor gas. The ion beam emitted by this source had an energy width of 3 eV [8] and was mass separated by an 80° deflection magnet before entering the main UHV chamber. The position of the ion beam ($\phi \sim 3$ mm) on the sample surface was monitored using a Faraday cup (ϕ 0.5 mm). The integrated image of the ion beam intensity profile on the sample was measured by spatially resolved XPS (analysis spot ϕ 0.8 mm) and used to calculate the ion fluence as a function of the measured ion implantation dose. The implantation was interrupted after certain fluences for in situ XPS (Mg K_α, 1253.6 eV) and Rutherford backscattering analysis (RBS) ($^4He^+$, 1 MeV, 165° scattering angle) analysis. The electrostatic analyser for XPS was operated at a constant pass energy of 23.5 eV. The photoelectrons were detected at 90° relative to the sample surface and the Au $4f_{7/2}$ core level line (84.0 eV) of a clean gold sample was used for energy calibration. The base pressure in the ARTOSS main UHV chamber and the pressure during analysis and ion bombardment stayed below 10^{-8} Pa.

In a separate experiment the weight change of a polished polycrystalline beryllium target during 3 keV CO^+ ion bombardment at normal incidence was measured using the high-current ion source described in [9]. The remaining carbon and oxygen impurity concentrations after polishing were in the range of $(5–10) \times 10^{16}$ cm^{-2}. The weight of the target was determined after certain ion doses using a Mettler 22 vacuum microbalance with a sensitivity <1 μg. The weight change was calculated in relation to the original sample weight measured before the ion bombardment in the same vacuum chamber. The base pressure in the target chamber was about 10^{-7} Pa, the pressure during ion bombardment about 10^{-4} Pa.

The Monte Carlo program TRIDYN (version 40.3) [10,11] was used to calculate the ion ranges and sputtering yields. This program takes into account all collisional effects such as implantation, reflection, and sputtering. Ions and collisional cascades are tracked until the respective particle energy falls below the surface binding energy of this particle in the target. These energies are based on the elemental heats of sublimation and are interpolated to take into account the surface composition of the target [12]. Chemical erosion, diffusion and segregation are not considered. Though the program is able to take changes in target composition due to the ion beam into account, this option was not used here because we wanted to obtain physical sputtering yields for a fixed target composition under simultaneous bombardment with two ion species.

3. Results and discussion

3.1. C^+ bombardment

The RBS analysis after the implantation steps shows a continuous increase of the deposited carbon amount with increasing fluence and this behaviour is well reproduced by TRIDYN computer simulations, as we recently reported elsewhere [6]. Depth profiles given by TRIDYN suggest that a carbon layer builds up on top of the beryllium substrate [6]. This adlayer formation is also confirmed by weight change measurements which show a continuous increase of the sample weight with increasing ion fluence [13]. This is also consistent with a carbon self sputtering yield below unity at normal incidence [14].

The fluence dependence of the surface composition, derived from the XPS measurements using the intensity ratios and the characteristic sensitivity factors of the different elements [15], confirms this model. The carbon share of the surface composition increases with fluence until it reaches almost 100% at a C^+ fluence of 111.7×10^{16} cm^{-2}. This means that a pure carbon adlayer builds up on the beryllium substrate because the probability for a photoelectron emitted at a certain depth to leave the sample decreases exponentially with depth (it can be estimated that $<5\%$ of the overall intensity comes from a depth >6 nm).

In addition to the elementary composition of the surface layer, XPS analysis gives information about the chemical composition of the growing adlayer. Fig. 1 shows the XPS spectra of the C 1s binding energy region after the denoted C^+ implantation fluences. For a fluence of 8.9×10^{16} cm^{-2} there is almost no carbon signal visible. This is due to the mean implantation depth of the carbon ions in beryllium (TRIDYN: 20 nm) which is beyond the reach of XPS. The increase of fluence then leads to a broadening of the implantation profile and simultaneously to erosion of beryllium at the surface. Because of these effects the implanted carbon is not visible for XPS until a fluence of 20.1×10^{16} cm^{-2}.

At this and at the next higher fluence the carbon signal is almost entirely located at a C 1s binding energy which is characteristic of Be_2C [16]. A second peak, originating from elementary carbon [17] is not observed until the C^+ fluence reaches a value of 42.4×10^{16} cm^{-2}. For higher fluences the elementary signal increases and dominates the spectrum more and more until only a small carbide signal is left at a fluence of 111.7×10^{16} cm^{-2}.

The observed behaviour can be explained by the following model: Directly after implantation of carbon into clean beryllium Be_2C is formed. With increasing deposited carbon amount and simultaneous beryllium sputtering the carbon fraction in the surface layer accessible by XPS exceeds the stoichiometric value of 33%

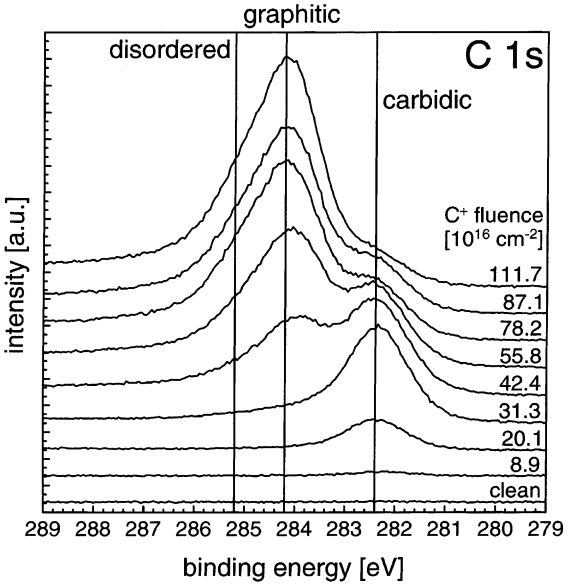

Fig. 1. XPS spectra of the C 1s binding energy region at the denoted C^+ fluences. The vertical lines indicate the peak positions for graphitic and disordered carbon and beryllium carbide.

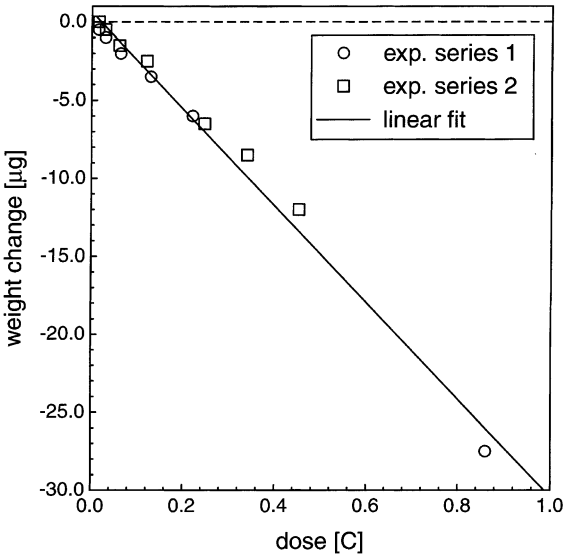

Fig. 2. Weight change of a polycrystalline beryllium target with 3 keV CO^+ dose. The solid line is the result of a linear fit including the two separate experimental series shown.

(41% at 42.4×10^{16} cm^{-2}). Therefore the carbon cannot completely be bound in Be_2C anymore. Eventually this leads to the sample structure of elementary carbon on top and Be_2C in the transition region between pure carbon and pure beryllium.

3.2. CO^+ bombardment

In the case of CO^+ bombardment the molecular ions split upon impact on the sample surface and the ion energy is divided between carbon and oxygen corresponding to their mass ratio of 3:4, thus simulating a co-bombardment of the sample with carbon and oxygen. We recently showed that in contrast to the C^+ bombardment the deposited amounts of carbon and oxygen are limited and a deposition/erosion equilibrium is established after a certain fluence.

Fig. 2 shows the weight change of a polycrystalline beryllium target during 3 keV CO^+ bombardment. Because the equilibrium is already established at the lowest dose shown in the graph (15 mC, RBS shows equilibrium after 0.5 mC) a linear fit is used to obtain a beryllium sputtering yield (see Table 1). Taking into account the fact that the total deposited amounts of carbon and oxygen do not change any more after equilibrium is reached (i.e., unity erosion yield for both elements) the whole weight loss must be due to a continuing beryllium erosion.

Table 1
Experimental and calculated (TRIDYN) erosion yields of beryllium, carbon and oxygen due to 5 keV CO^+ bombardment[a]

	Be	C	O
TRIDYN	0.36	0.24	0.29
Experimental	0.33	1.00	1.00

[a] In the calculations a homogeneous target containing 40% O, 32% C and 28% Be is assumed.

The chemical composition of the ternary surface layer can be derived from the XPS binding energy spectra of the Be 1s and C 1s regions. Fig. 3 shows the XPS spectra of the C 1s region after the denoted CO^+ fluences. Besides the contributions from disordered and graphitic carbon, Be_2C and a broad intensity band at values above the energy characteristic for disordered carbon are observed. These last signals cannot be attributed to a single compound but can be generally assigned to C–O compounds like CO, CO_2 or carbonates whose binding energies are known to lie in the marked region [18,19]. While the beryllium carbide signal decreases and eventually vanishes with increasing fluence, the C–O compound intensity increases and reaches a saturation level after equilibrium is reached. This means that inside the ternary mixture layer after implantation carbon is bound to a certain extent in C–O compounds directly after implantation.

While it is not possible to fit the C 1s signal due to the contribution of the C–O compounds, the Be 1s XPS spectra were fitted using the MultiPak V 5.0 A code (Physical Electronics). For this fitting procedure (least

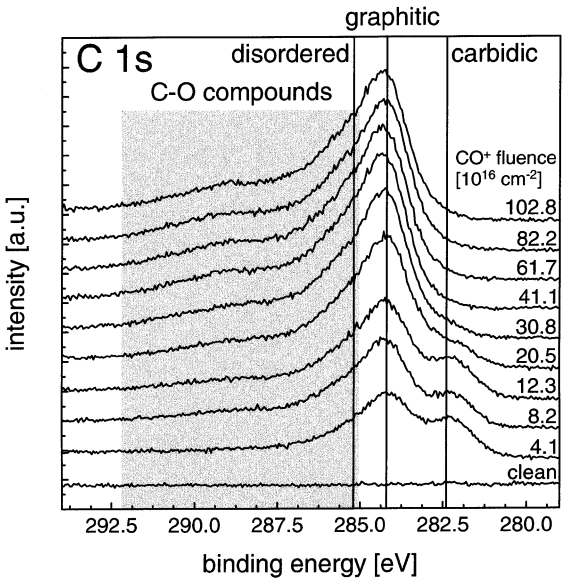

Fig. 3. XPS spectra of the C 1s binding energy region at the denoted CO^+ fluences. The vertical lines indicate the peak positions for graphitic and disordered carbon and beryllium carbide. The grey rectangle marks the known energy region for a number of simple C–O compounds.

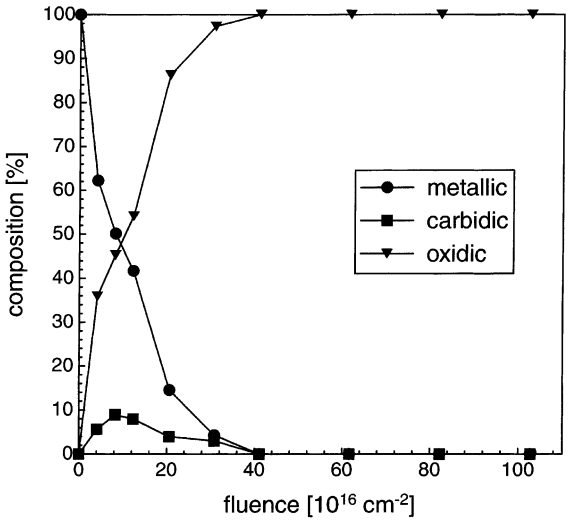

Fig. 4. Composition of the Be 1s XPS signal at the different CO^+ implantation fluences. For the fitting procedure binding energies of metallic beryllium, BeO and Be_2C according to [16,19] have been used.

square fit) each contribution is approximated by a combined, symmetric Gaussian/Lorentzian function centered at its characteristic binding energy. A Shirley-type background subtraction was applied to the spectra before the actual fitting procedure. The results of these fits are shown in Fig. 4. Again there is a Be_2C signal only before the equilibrium is established. After the equilibrium is reached the beryllium in the ternary layer is completely bound in beryllium oxide. At equilibrium the ternary surface layer is composed of BeO, elementary carbon and C–O compounds, no beryllium carbide is detected (enthalpy of formation: BeO:- 612.5 kJ/mol, Be_2C:- 117.0 kJ/mol [20]).

The equilibrium surface composition of the sample can be calculated from XPS spectra in the same way as described in Section 3.1. It results in 40% oxygen, 32% carbon and 28% beryllium. Because of the mentioned photoelectron attenuation, this composition would be valid for a homogeneous surface layer only. However, this composition can be used as an approximation together with the total difference in the deposited carbon and oxygen equilibrium amounts measured by RBS (oxygen: 9×10^{16} cm^{-2}, carbon: 8×10^{16} cm^{-2}). Assuming furthermore densities of 2 g cm^{-3} for carbon and 3 g cm^{-3} for BeO, an estimated homogeneous layer of the quoted composition must be 12 nm thick to agree with both the XPS and RBS results. Because the calculated mean implantation depths (TRIDYN: 8 nm) and implantation profiles for both elements are almost identical and because only the first 6 nm are relevant for XPS, the difference in the total amounts must be explained by an inhomogeneous layer composition near the sample surface. Thus it can be concluded that the ternary surface layer is not homogeneous and that the uppermost surface is rich in oxygen compared to carbon (BeO at the surface, C chemically eroded). The concentrations of carbon and oxygen decrease and become almost equal as the sample depth increases.

However, using the composition measured by XPS as an approximation the physical sputtering yields of carbon, beryllium and oxygen due to 5 keV CO^+ bombardment can be calculated by TRIDYN for equilibrium conditions (see Table 1). Beryllium is bound in BeO only and the BeO enthalpy of sublimation has been used for the TRIDYN calculations. Therefore the particle energy below which TRIDYN stops to calculate the further particle path is correct in the case of beryllium. Comparing the experimental and the calculated beryllium value, they are almost identical. Thus it can be concluded that beryllium is eroded by physical sputtering only. For carbon and oxygen the experimental and the TRIDYN values are clearly different. Here the presence of C–O compounds in the sample must be considered. While a crystal lattice usually has a binding energy of several eV, molecules like CO or CO_2 do not form such a lattice and they have adsorption energies on surfaces which are generally below 1 eV. The assumption of a BeO lattice with stored and adsorbed C–O compounds thus explains a much easier and thus higher erosion of oxygen and carbon which cannot be calculated by TRIDYN because of the too low surface

binding energies compared to the mentioned interpolation. Additionally, the impinging ions can break existing bonds and enable the formation of molecules like CO directly at the surface. In this case even the enthalpy of formation supplies enough energy for desorption ($C + O \rightarrow CO$: ~1.1 eV). Taking into account that the physical sputtering yields of oxygen and carbon are quite similar (see Table 1) and that the overall erosion yield is one for both elements it is probable that the observed chemical erosion is due to the desorption of carbon monoxide molecules.

4. Conclusions

Models have been constructed for the build-up of mixed layers on a beryllium substrate and the erosion of the target during 5 keV C^+ and 5 keV CO^+ bombardment, respectively.

In the case of C^+ implantation an elementary carbon layer builds up on top of a transition region containing beryllium carbide between pure carbon and pure beryllium. Beryllium erosion stops after the development of a shielding carbon layer.

In the case of CO^+ bombardment an erosion/deposition equilibrium is established and an approximately 8 nm thick ternary mixture layer containing beryllium, carbon and oxygen forms on top of the substrate. The composition of this layer is not homogeneous. While the surface is relatively rich in oxygen compared to carbon, the concentration of these two elements approaches a similar value with increasing sample depth. In the ternary mixture layer beryllium is entirely bound in beryllium oxide. Carbon is present as a mixture of elementary carbon and C–O compounds. There is no Be_2C. Beryllium erosion does not stop and is due to physical sputtering by the impinging CO^+ ions with a sputtering yield of 0.33. For carbon and oxygen we suggest a chemical erosion process which takes place via the desorption of carbon monoxide molecules.

References

[1] ITER Project, Detailed Design Document, IdoMS#G 16 DDD 2 96-11-27 W 0.2, 1996.
[2] The JET Team: presented by P.R. Thomas, J. Nucl. Mater. 176&177 (1990) 3.
[3] R. Satori, G. Saibene, D. Goodall, E. Usselmann, P. Coad, D. Holland, J. Nucl. Mater. 176&177 (1990) 624.
[4] P. Rebut, M. Hugon, S. Booth, J. Dean, K. Dietz, K. Sonnenberg, M. Watkins, JET-R(85)03, JET Joint Undertaking, Abingdon, 1985.
[5] E. Bertolini, Fus. Eng. Des. 27 (1995) 27.
[6] P. Goldstrass, W. Eckstein, Ch. Linsmeier, J. Nucl. Mater. 266–269 (1999) 581.
[7] Ch. Linsmeier, K.U. Klages, P. Goldstrass, Physica Scripta, submitted.
[8] R. Aratari, W. Eckstein, Nucl. Instrum. and Meth. B 42 (1989) 11.
[9] W. Eckstein, C. Carcia-Rosales, J. Roth, W. Ottenberger, Sputtering Data, IPP-Report 9/82, 1993.
[10] W. Eckstein, Computer Simulation of Ion–Solid Interaction, Springer, Berlin, 1991.
[11] W. Möller, W. Eckstein, J. Biersack, Comput. Phys. Commun. 51 (1988) 355.
[12] W. Eckstein, M. Hou, V.I. Shulga, Nucl. Instrum. and Meth. B 119 (1996) 477.
[13] E. Gauthier, W. Eckstein, J. Laszlo, J. Roth, J. Nucl. Mater. 176&177 (1990) 438.
[14] J. Roth, J. Bohdansky, W. Ottenberger, J. Nucl. Mater. 165 (1989) 193.
[15] D. Briggs, M. Seah, Practical Surface Analysis by Auger and X-ray Photoelectron Spectroscopy, Wiley, Chichester, 1983.
[16] P. Goldstrass, Ch. Linsmeier, Nucl. Instrum. and Meth. B 161–163 (2000) 411.
[17] J. Luthin, Ch. Linsmeier, Surf. Sci. 454–456 (2000) 78.
[18] Meyer, E. Reinhart, D. Borgmann, G. Wedler, Surf. Sci. 320 (1994) 110.
[19] Moulder, et al., Handbook of X-ray Photoelectron Spectroscopy, Physical Electronics Inc, Eden Prairie Minnesota, 1995.
[20] I. Barin, Thermochemical Data of Pure Substances, vol. 1, third ed., VCH, Weinheim, 1995.